

THE BUBBLE CLOSE-OFF DENSITY OF ICE IN ANTARCTIC ICE SHEETS

Akira HIGASHI, Masayoshi NAKAWO and Hiroyuki ENOMOTO

*Department of Applied Physics, Faculty of Engineering, Hokkaido University,
Kita-13, Nishi-8, Kita-ku, Sapporo 060*

Abstract: Measuring methods of the density and the total gas content in ice cores were developed considering various sources of systematic errors. The special attention was forwarded to the method of correction for the effect of surface-exposed air bubbles. True density ρ_t and the total gas content R were obtained for ice cores drilled at three sites (S 48, H 231 and Z 102.5) of different altitudes in the Sôya drainage basin and the Shirase drainage basin, East Antarctica. The bubble close-off densities ρ_c calculated from obtained data with an appropriate assumption of particle paths exhibit their increasing tendency with increasing elevation of the sites of close-off. The relationship between the reduced void ratio a_c and the temperature T_c , both at the close-off, exhibits a little higher level with almost the same gradient than the result obtained by RAYNAUD and LABEL (Nature, **281**, 289, 1979).

1. Introduction

Importance of the deep ice core as a bearer of climatic records is now widely recognized and many projects of drilling deep cores were carried out in Greenland and Antarctica. Most important and popular clue remaining in ice is $\delta^{18}\text{O}$ with which many papers were already published. Recently inclusions in ice (volcanic ash and microparticles), acidity and NO_x content are attracting attentions. In addition to these chemical aspects, physical properties of the ice core such as the density, the fabrics and the total gas content have become the subjects of interest.

Air bubbles in ice close off at a certain density being separated from channels that were connected to the firn in the process of deposition. If the mass of air in ice is kept without diffusion, no matter how it is compressed or deformed due to the deposition and flow, the total gas content (volume of air at standard temperature and pressure in unit mass of ice) should be kept constant at a value to be determined by temperature and atmospheric pressure of the site of close-off. Using this notion, we can estimate the place of origin of the ice core by accurate measurements of the total gas content. If we can estimate the origin of ice cores at any depth, we can analyze more precisely the temperature data furnished by the depth profile of $\delta^{18}\text{O}$, distinguishing the variation due to the climatic change and that caused by the flow of ice from higher altitude.

This paper describes our preliminary work on the accurate measurements of the density and of the total gas content in ice cores from Antarctica. We paid very careful attention to the systematic errors accompanying our methods of measurements

and found the importance of the surface area correction. Although the depth of ice cores is limited only down to 113 m, interesting results were obtained in view of our purpose of the study stated above. Altitude dependence of the bubble close-off density ρ_c calculated from obtained data of the true density ρ_t and the total gas content R is clearly shown. This may imply that the void ratio formed at the close-off is temperature dependent.

2. Experimental Methods

2.1. Density measurements

Densities were measured by the hydrostatic method using isooctane as the immersion liquid. The standard procedures of the measurement for ice were described by LANGWAY (1958) and NAKAWO (1980). An electronic balance (minimum sensitivity 0.01 g) and a quartz thermometer were used for quick and accurate measurements of weight and temperature respectively. The density can be determined by the following equation,

$$\rho_s = \frac{M}{V} = \frac{\rho_l W_a - \rho_a W_l}{W_a - W_l}, \quad (1)$$

where W_a is the weight of a sample in air, W_l the weight in liquid, ρ_l and ρ_a are the density of liquid and air respectively. Since the required accuracy of the density of the ice core is in the order of 0.01 kg/m^3 , the density of the immersion liquid should be well known as a function of temperature. This was determined by using eq. (1) with the known density of good quality ice single crystals from the Mendenhall Glacier, Alaska stored in our laboratory. Temperature dependence of the density of the standard ice from the Mendenhall Glacier is given by BADER (1964) as,

$$\rho_i = 0.91650 \{1 - 10^{-6} T(157.556 + 0.2779T + 0.008854T^2 + 0.0001778T^3)\}. \quad (2)$$

From many measurements between -12°C and -16°C , a good linear relationship was obtained as follows,

$$\rho_i = 708.35 - 0.780T_l, \quad (3)$$

in which the unit of the density is $\text{kg}\cdot\text{m}^{-3}$ and that of liquid temperature T_l is $^\circ\text{C}$.

Temperature dependence of the air density ρ_a ($\text{kg}\cdot\text{m}^{-3}$) can be obtained by the standard formula,

$$\rho_a = \frac{1.293}{1 + 0.00367T_a} \frac{P_a}{1013}, \quad (4)$$

where T_a is the air temperature ($^\circ\text{C}$) and P_a the atmospheric pressure (in mb) under which the measurements were carried out. Temperature was measured by a quartz thermometer of an accuracy of 0.001°C . Since the errors in calculations of ρ_l and ρ_a by eqs. (3) and (4) are very small owing to the accurate temperature measurements, the error in the determination of ρ_s by eq. (1) principally comes from a relative error of the weight measurements which is in the order of 10^{-4} . This means that the error in the density is approximately $0.1 \text{ kg}\cdot\text{m}^{-3}$ although it is numerically calculated to the order of $0.01 \text{ kg}\cdot\text{m}^{-3}$.

2.2. Total gas content

The apparatus used for the measurement of the total gas content in ice cores is almost the same as the one employed by LANGWAY (1958). Ice sample of which density and mass were accurately determined was immersed in kerosine filled in a beaker in the cold room. After covering the top of the sample with an inverted glass funnel connected to a burette, both also filled with kerosine, the apparatus was removed into a laboratory at a temperature approximately 5°C. As the sample melted, the segregated air rose in kerosine and displaced that at the top of burette. The whole amount of the air released during the melting was collected in the top part of the burette. The burette was graduated into 0.05 cm³ divisions wide enough to interpolate accurately to approximately 0.01 cm³. The measured volume of the air in the burette was converted into that at standard pressure and temperature (SPT; 1 atm. and 0°C) by using eq. (4), considering the air pressure in the burette determined from atmospheric pressure in the laboratory and its temperature.

The measured volume of air by the burette should contain the vapor of kerosine because it is entrained into the air bubbles during their rising in the kerosine. Since the amount of entrained kerosine is considered to be proportional to the released air volume, the corrections proportional to the measured volume should be subtracted. The correction factor 8% was obtained by a simple experiment of measuring the density and air volume by the melting of an artificially made bubbly ice as will be described below.

A small cylindrical cavity was perforated in a single crystal specimen by a small drilling machine and it was choked with a piece of ice at the end to make an isolated cavity in the specimen. At first the density of this specimen was measured by the hydrostatic method and then it was melted in the apparatus of the gas content measurements. The volume u of the artificial cavity can be calculated by

$$u = V \left(1 - \frac{\rho_s}{\gamma_i} \right), \quad (5)$$

where V is the specimen volume, ρ_s the density of the specimen and γ_i the density of pure ice. The air volume measured by the melting method was larger than the above u by the amount of entrained kerosine vapor. The difference was approximately 8% of the air volume V_a measured by the burette. Therefore, the kerosine vapor correction was 8% reduction of V_a .

Since a small amount of air should be dissolved into the melt water during the process of melting, it is necessary to add this amount to evaluate the total gas content in ice. Dissolved air content was evaluated from the measured value of the oxygen content in the melt water deposited at the bottom part of the beaker. The oxygen content was measured by a modified Winkler method. Specimen water was collected by a syringe from the beaker when it was cold (approximately 5°C) to avoid supersaturation.

Results of the measurement of O₂ in specimens of several ice cores indicate that they dissolve O₂ approximately 93% of the saturated value in ice. As was pointed out by LANGWAY (1958), ice cores from Antarctica are almost saturated with O₂ and hence with air. However, even the pure ice, such as single crystals from the

Mendenhall Glacier, contains O_2 approximately 55% of the saturated value. This is in accordance with the previous result of dissolved O_2 in the Mendenhall ice obtained by HIGASHI and HASHIMOTO (1961). Therefore, it is inferable that the amount of the air entrained into the melt water during the melting of specimens should be approximately $93 - 55 = 38\%$. Since the saturated value of air in pure water is $29 \text{ cm}^3/\text{kg}$ at 0°C , the correction for the dissolved air in water is estimated approximately $29 \times (38/100) \simeq 11 \text{ cm}^3/\text{kg}$. This dissolved air correction proportional to the mass of specimen should be added after making the kerosine vapor corrections and the surface area corrections. The surface area correction will be explained in the next subsection in detail, because it is associated with the density measurement as well as the total gas content.

2.3. Effect of the specimen size

In the present case of the density measurement of ice cores which contain many air bubbles, measured volume of the specimen is evaluated less than the geometrical volume shaped by the plane because the half-cut air bubbles exposed on the surface are filled with the immersion liquid. Therefore, the density is evaluated larger than the real if we use a specimen of which surface/volume ratio is large. This effect also gives smaller values for the total gas content than the real.

Correction for the effect of specimen size can be evaluated as follows. The real density of ice ρ_t and the measured one by the hydrostatic method ρ_s are related in the following way;

$$M = \rho_s V = \rho_t (V + v), \quad (6)$$

where M is the mass of ice, V the measured volume of ice and v the volume of bubbles exposed to the surface. Since v is considered to be proportional to the specimen surface area S , the correction factor α can be defined as

$$v = \alpha \cdot S, \quad (7)$$

and therefore α has a dimension of length. From eqs. (6) and (7), we obtain

$$\frac{V}{S} = \frac{1}{\rho_t} \left(\frac{\rho_s V}{S} \right) - \alpha. \quad (8)$$

The real density, ρ_t and α can be estimated from a diagram of the relationship between V/S and $\rho_s V/S$ which can be obtained from density measurements with many specimens of different ratio of V/S . For the exact measurement of S , specimens were cut and shaped by a plane into a parallelepiped shape as exact as possible and lengths of its sides were measured by a calliper.

One example of the estimate of ρ_t and α is given in Fig. 1 in which the relationships between V/S and $\rho_s V/S$ for Mizuho No. 132 specimens are plotted. Values of ρ_t and α given in the figure were calculated with the least squares method using eq. (8) and many data as plotted in Fig. 1. Diagrams as Fig. 1 for various ice cores of different densities were drawn and ρ_t and α were calculated in the same way. The correction factor α should be a function of the porosity or the density, as to be expected $\alpha=0$ for bubble-free ice. The surface correction for the total gas content in ice is given by eq. (7) knowing the surface area S of the individual specimen.

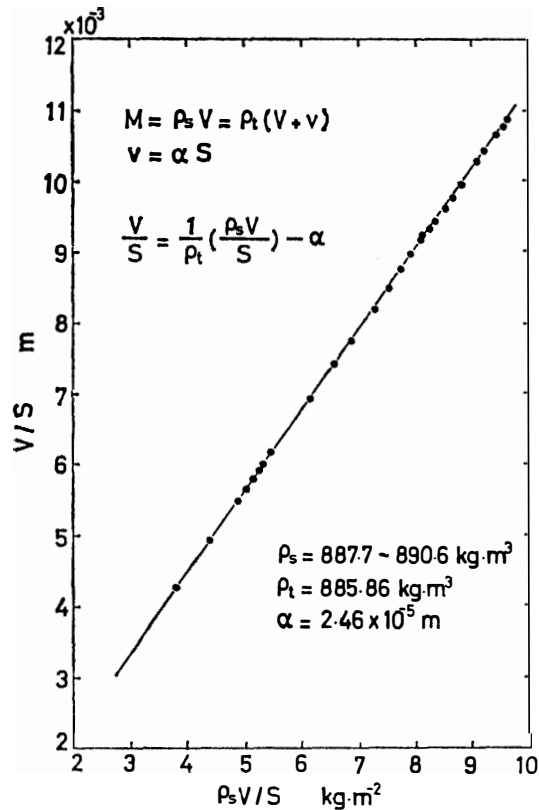


Fig. 1. A diagram used to determine true density ρ_t from many measurements of ρ_s with specimens of different values of V/S . ρ_t is given by the reciprocal of the inclination of the straight line and the surface correction factor α is calculated with the least squares by a standard equation shown in the figure.

3. Results of Measurements

3.1. Densities of ice

Specifications of ice cores examined in the present study are tabulated in Table 1. The mean value of the depth of upper and lower ends of each core in the table is taken as the depth of core. Several specimens were cut from those cores of which length ranged 20–70 cm. Locations of the drilling sites are shown in a map of Fig. 2. S 48 is in the continuous accumulation zone (YAMADA and WAKAHAMA, 1981) where a comparatively large amount of snow accumulates homogeneously ($>20 \text{ g}\cdot\text{cm}^{-2}\cdot\text{a}^{-1}$). H 231, Z 102.5 and Mizuho are all in the sporadic accumulation zone where occasional absence of the annual accumulation layers is observed. The accumulation rate in this zone is as low as in the order of $10 \text{ g}\cdot\text{cm}^{-2}\cdot\text{a}^{-1}$ or less and it is quite difficult to determine the rate exactly because of local fluctuations.

Except those at Mizuho Station, all cores were obtained from bore holes for seismic explosion tests drilled by mechanical drilling machines which were developed for this purpose (SUZUKI and SHIRAISHI, 1982). The Mizuho cores were drilled by a thermal drilling machine developed for the intermediate depth drilling project (SUZUKI and TAKIZAWA, 1978).

Densities of individual ice cores ρ_t (at -15°C) obtained by the method described in the preceding Subsection 2.3 are tabulated in Table 1. Depth profiles of ρ_t are illustrated in Fig. 3, in which the data at different sites are designated by different symbols indicated as legends in the figure. Upper and lower limits of measured data

Table 1. Specification of ice cores from Mizuho Plateau, Antarctica.

Exp. No.	Core No.	Depth (m)	Site No. (elevation)	Date of drilling (Number of expedition)	True ρ_t density of ice core at -15.4°C ($\text{kg}\cdot\text{m}^{-3}$)
1	187	61.56– 61.77	S 48 (1200 m)	Jan. 1979 (JARE-20)	862.70
2	175	57.58– 57.67			835.48
3	155	51.42– 51.57			820.08
4	120	56.80– 57.02	H 231 (1667 m)	Oct. 1980 (JARE-21)	845.07
5	141	68.16– 66.55			875.82
6	184	81.32– 81.63			888.40
7	228	99.72– 99.90	Z 102.5 Mizuho	Z 102.5 Oct.–Nov. 1980 (JARE-21)	902.50
8	102	55.27– 55.57			873.90
9	108	59.89– 60.41			867.84
10	118	60.50– 60.70	Z 102.5 (2212 m) Mizuho	Mizuho Jan. 1975 (JARE-15)	882.40
11	144	70.10– 70.40			894.70
12	132	72.12– 72.57			885.86
13	171	80.35– 80.45	Z 102.5 Mizuho		898.40
14	198	90.79– 90.90			903.42
15	143	97.98– 98.73			901.80
16	225	100.32–100.60	Z 102.5		905.30
17	261	112.90–113.40			909.50

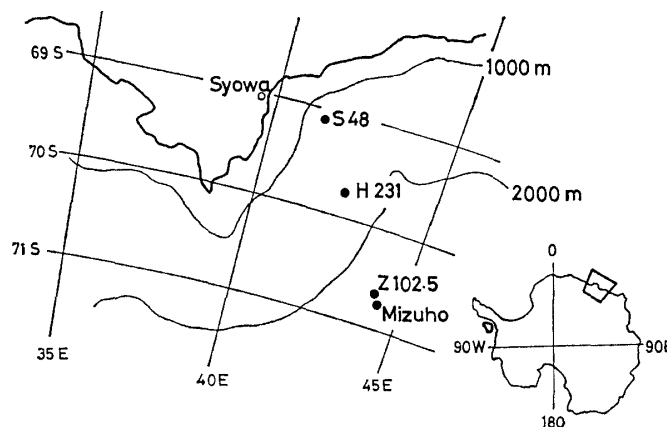


Fig. 2. A map to show the sites of drilling (see Table 1).

ρ_s are plotted with filled symbols and calculated values of true density ρ_t were plotted by open symbols. Effects of the surface-exposed bubbles are clear in data of small ρ_s as those of shallow depth of S 48.

Difference of the density profile between H 231 and Z 102.5 should be due to the different modes of snow accumulation at these sites: accumulation rate is estimated approximately $15 \text{ g}\cdot\text{cm}^{-2}\cdot\text{a}^{-1}$ at the former whereas less than $10 \text{ g}\cdot\text{cm}^{-2}\cdot\text{a}^{-1}$ at the latter (YAMADA and WAKAHAMA, 1981). The fact that the profile is different between Z 102.5 and Mizuho although they are quite near and at almost the same elevation could be explained by the difference in relaxation after the cores were drilled (see the data of excavations in Table 1).

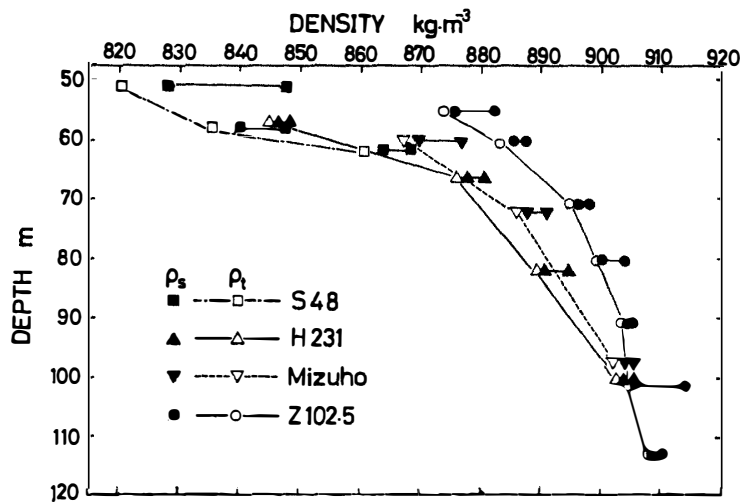


Fig. 3. Depth profiles of the true density ρ_t of ice cores at different drilling sites.

3.2. Total gas content

Data of the volume of air in ice V_a measured by the method of melting (at STP) for individual cores and evaluated corrections described in the preceding section are tabulated in Table 2 together with necessary data. Although two or three measurements were made for every core, tabulated data are those of large volume with smaller values of surface/volume ratio. The surface correction factor α obtained in the procedure of determining the true density ρ_t as described in Subsection 2.3 is tabulated in Table 2 together with the mass M and the surface area S of every specimen.

Table 2. Evaluations of total gas content from the measured volume of air.

Experiment No. (left) and Sample No. (right)	V_a Measured volume of air, STP (cm ³)	M Mass of specimen (g)	S Surface area of specimen (cm ²)	α Surface correction factor (10 ⁻³ cm)	$S\alpha=v$ Surface correction (cm ³)	Kerosine vapor correction (cm ³)	Dis-solved air correction (cm ³)	V_a' Cor-rected vol. of air (cm ³)	R Total gas content (cm ³ /kg)
1	187	256.98	271.4	4.5	1.22	2.30	2.81	30.51	118.7
2	175	134.64	185.1	5.9	1.09	1.28	1.48	17.38	129.1
3	155	213.92	250.4	11.2	2.80	2.31	2.35	31.66	148.0
4	120	219.52	247.0	6.0	1.48	1.88	2.41	25.45	115.9
5	141	213.58	227.9	2.3	0.52	1.67	2.35	22.10	103.5
6	184	250.35	259.7	1.8	0.46	2.18	2.75	28.22	112.7
7	228	223.39	235.7	0.5	0.12	1.80	2.46	23.31	104.3
8	102	222.17	242.2	3.7	0.10	1.91	2.44	24.54	110.4
9	108	110.64	160.8	2.9	0.47	0.63	1.22	8.91	80.5
10	118	225.06	229.3	2.3	0.52	1.13	2.47	16.03	71.3
11	144	156.04	190.3	1.3	0.25	0.88	1.72	12.03	77.1
12	132								
13	171	197.95	217.9	1.0	0.22	1.67	2.18	21.65	109.3
14	198	111.79	161.3	0.5	0.08	0.94	1.23	12.13	108.5
15	143	150.95	207.1	0.4	0.08	1.20	1.66	15.51	102.7
16	225	122.78	161.7	0.3	0.05	0.88	1.35	11.46	93.3
17	261	120.12	193.2	0.03	0.01	0.96	1.32	12.42	103.4

The calculated surface correction terms $v=S\alpha$, the kerosine vapor correction terms -8% of the V_a and the dissolved air correction terms $11 \text{ cm}^3/\text{kg}$ of the mass of ice are consecutively tabulated in Table 2. Real volume of air existing in the specimen is tabulated in a column of V_a' and the total gas content is obtained as $V_a'/M=R$ in the last column.

Depth profiles of the total gas content are shown in Fig. 4. Values for the cores No. 108, 118 and 144 are all much smaller than others of approximately the same depths. Although it can be justified to exempt No. 108 because it is a core obtained several years prior to others at Mizuho, we have no explanation why Nos. 118 and 144 are so deviated. However, if we also exempt those two points, a straight solid line can be drawn among the plotted data for both sites H 231 and Z 102.5. This relationship, the decreasing tendency of the total gas content with increasing depth, will be discussed in the next section. Another straight line (chain line in the figure) can be drawn through three data points for the site S 48, but it has a much steeper slope against the depth than that described above. For the case of the site S 48, the ice at the depths above 60 m is probably not completely closed-off as could be anticipated from the density profile of Fig. 3.

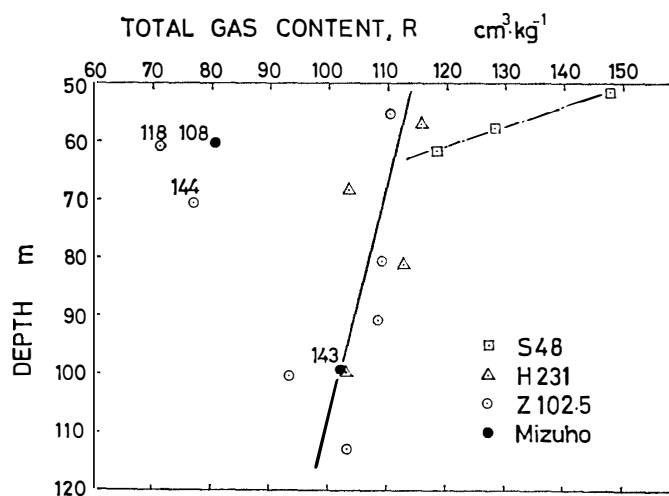


Fig. 4. Depth profiles of the total gas content R of ice cores at different drilling sites.

3.3. Bubble pressures

The bubble pressure, that is to say, the pressure of air contained in enclosed isolated bubbles in original ice cores can be evaluated from the density and the total gas content determined as in the preceding subsections. The bubble pressure P_s is equal to the ratio of the volume of air expelled from the bubbles on melting converted into the standard condition V_a' to that of the voids V_v at 0°C , and it can be calculated by the following equation,

$$P_s = \frac{V_a'}{V_v} = \frac{R}{(1/\rho_t - 1/\gamma_s)}, \quad (9)$$

where γ_s is the density of pure ice at a temperature of density measurement and R is the total gas content shown in the last column of Table 2. V_v is converted from the

value calculated for the measuring temperature (-15°C) into 0°C by multiplying the temperature ratio.

Calculated results of P_s for individual cores are tabulated in Table 3 which also shows necessary data for the evaluation of the close-off density and results to be described in the next section. Depth profiles of the bubble pressure for three drilling sites are shown in Fig. 5. Inclinations of the increase of bubble pressures with increasing depth are almost the same for H 231 and Z 102.5. The overburden pressure of

Table 3. Evaluations of the close-off densities according to eq. (13).

Exp. No. (left) and Sample No. (right)	ρ_t True density of ice core (kg/m^3)	H_c Elevation of close-off (m)	P_c Atmospheric pressure at H_c (atm.)	P_s Bubble pressure (atm.)	a_s Void ratio at T_s (cm^3/kg)	ρ_c Close-off density (kg/m^3)
1 187	862.70	1217	0.817	1.58	70.9	817.9
2 175	835.48	1213	0.817	1.12	108.6	810.3
3 155	820.08	1207	0.817	1.06	131.1	796.8
4 120	845.07	1644	0.778	1.16	94.0	817.5
5 141	875.82	1648	0.778	1.83	53.5	827.8
6 184	888.40	1653	0.777	2.85	37.3	820.6
7 228	902.50	1661	0.776	4.99	19.7	827.2
8 102	873.90	2203	0.731	1.90	56.0	819.3
9 108	867.84	2224	0.729	1.19	64.0	845.9
10 118	882.40	2207	0.730	1.50	44.9	853.8
11 144	894.70	2213	0.736	2.47	29.4	849.6
12 132	885.86	2233	0.728			
13 171	898.40	2221	0.729	4.16	24.8	821.9
14 198	903.42	2226	0.729	5.51	18.6	822.4
15 143	901.80	2247	0.727	4.71	20.6	827.1
16 225	905.30	2230	0.729	5.39	16.3	835.2
17 261	909.50	2236	0.728	8.69	11.2	826.8

$T_s = -15.4^{\circ}\text{C} = 257.8\text{ K}$. T_c for S 48 = 253.4 K. T_c for H 231 = 247.8 K. T_c for Z 102.5 = 238.6 K ~ 239.0 K according to elevations. $\gamma_s = 918.9\text{ kg}/\text{m}^3$ at 257.8 K.

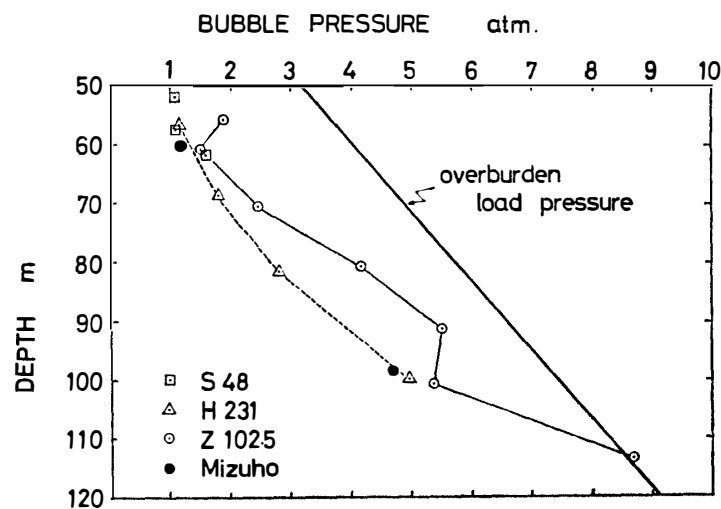


Fig. 5. Depth profiles of the bubble pressure P_s of ice cores at different drilling sites.

snow and ice at Mizuho calculated from the overall density profile (MAENO, 1982) is shown by a bold solid line in the figure.

4. Discussion

4.1. Close-off density

When the firn on an ice sheet transforms into ice due to the overburden pressure, air bubbles are separated from channels that are connected to the free surface of the firn. The separation or the isolation of all bubbles in ice is called the close-off and the density of ice at the close-off is the close-off density ρ_c . If we assume that the mass of air trapped in isolated bubbles is invariant irrespective of the change of volume due to the overburden pressure, there holds the following equation,

$$\frac{P_s a_s}{T_s} = \frac{P_c a_c}{T_c}. \quad (10)$$

In this equation, physical quantities (pressure P , temperature T and void ratio a , that is bubble volume per unit mass of ice) are specified by suffices s and c for the core sample and for the place where the sample closed off. The void ratio a_s and a_c are given by the following equations,

$$a_s = \frac{1}{\rho_t} - \frac{1}{\gamma_s}, \quad (11)$$

$$a_c = \frac{1}{\rho_c} - \frac{1}{\gamma_c}, \quad (12)$$

in which γ_s and γ_c are the densities of pure ice at a temperature of the density measurement and of the place of the close-off respectively. Then, combining eqs. (10), (11) and (12), we can obtain the close-off density ρ_c as follows,

$$\rho_c = \frac{\gamma_c}{(P_s T_c / P_c T_s) a_s \gamma_c + 1}. \quad (13)$$

Since P_s , the bubble pressure in individual cores, was obtained as tabulated in Table 3 from the total gas content and the density by eq. (9), ρ_c can be estimated by this equation if we know P_c and T_c . If there is no horizontal flow of ice at the site of drilling (e.g. top of the ice dome), we can evaluate T_c conversely by this equation from the value of ρ_c obtained from continuous density measurements of ice cores.

In the present case, since every drilling site is in the midstream of ice sheets of the Shirase basin and of the Sôya Coast, there are horizontal flows in the order of $10 \text{ m} \cdot \text{a}^{-1}$ or more (SHIBUYA and ITO, 1983). Therefore, the close-off for individual cores should have taken place at different sites upstream depending on the depth of cores and the velocity of ice.

Since there is an anticipation that ρ_c is a function of the elevation where the close-off takes place, we tried to evaluate ρ_c of all samples seeking their place of origin. The origin of ice or the site of close-off for a certain core can be determined if the particle path passing the depth of the core could be traced back upstream to the depth of close-off. Then, P_c and T_c necessary for evaluating ρ_c by eq. (13) could be estimated roughly

as the atmospheric pressure and the annual mean air temperature at this site.

Exact particle paths in ice sheets of our concern are not known yet, but the origin of an ice sample at a certain depth could be determined approximately using the elapsed time from the close-off and the horizontal velocity of ice. In the present case of shallow depth in an accumulation zone with the gentle surface slope, the elapsed time could be estimated from the difference in cumulative mass of overburden on a designated core and at the depth of close-off divided by the accumulation rate at the site of drilling cores. This approximation can be applied only when the following conditions are satisfied; (1) the vertical component of ice velocity is primarily constituted by the net accumulation and (2) the horizontal distance between the drilling site and the origin of ice is not too far to assume the same accumulation rate at both sites. The difference in cumulative mass of overburden could be estimated from such depth-density curves in Fig. 3.

It is known that the accumulation rate at Mizuho Station and its vicinity (including Z 102.5) is approximately $70 \text{ kg} \cdot \text{m}^{-2} \cdot \text{a}^{-1}$ on an average (YAMADA and WATANABE, 1978). Assuming that the depth of close-off is 50 m from the surface in this region (see Fig. 4), the difference of cumulative mass of overburden for a sample at a certain depth can be estimated by integration of the depth-density curve of Z 102.5 or more easily from a table provided for the Mizuho cores by NARITA and MAENO (1978). For example, the elapsed time for a sample of core No. 261 (113 m depth at Z 102.5) is calculated as follows,

$$(97523 - 34005) \div 70 = 907 \text{ (years)} . \quad (14)$$

Since the horizontal velocity of ice at Mizuho Station is approximately $14 \text{ m} \cdot \text{a}^{-1}$ (NARUSE, 1978), the horizontal distance between the drilling site and the origin of ice core No. 261 is approximately $14 \times 907 = 12698 \text{ m} \approx 12.7 \text{ km}$. This distance gives the elevation difference approximately 74 m, with the use of maximum surface slope 5.8 m/km along Y' route from Mizuho Station (WATANABE, 1977). Numerical values in the above calculation show that conditions (1) and (2) for approximation stated in the preceding paragraph can be satisfied.

Therefore, the elevation of the close-off of this sample is calculated as $2212 - 50 + 74 = 2236 \text{ m}$. Similar calculations were carried out with all samples except No. 12. Values for the accumulation rate for the cores at H 231 and S 48 were 160 and $250 \text{ kg} \cdot \text{m}^{-2} \cdot \text{a}^{-1}$ deduced from Fig. 5a of YAMADA and WATANABE's paper (1978). Those larger values made the elapsed time shorter than the case of Mizuho or Z 102.5. However, the increase of the surface slope at those sites made the elevation difference in the same order as above. Thus calculated elevations of the close-off for all samples are tabulated under a column H_c in Table 3. It should be noted, however, that the values of H_c could vary in the order of tens of meters because of the very large standard deviations which accompanied the accumulation rates used in the calculation.

The pressure P_c was calculated by the ordinary altitude dependence of atmospheric pressure ($-9.2 \times 10^{-2} \text{ mb} \cdot \text{m}^{-1}$) and the standard value at Mizuho Station (734 mb). The temperature T_c was obtained from the mean annual temperature -33°C at Mizuho (INOUE *et al.*, 1977) and the lapse rate there ($-1.3 \times 10^{-2} \text{ }^\circ\text{C} \cdot \text{m}^{-1}$, SATOW, 1978). The values of P_c for every core are tabulated in Table 3. Since the altitude

dependence of T_c is smaller than that of P_c , the values of T_c are given under the table for different drilling sites. γ_c is evaluated by eq. (2) according to T_c obtained above. The values of the close-off densities calculated by eq. (13) using those data in Table 3 are in the last column of the table and they are plotted against the elevation in Fig. 6. As stated in the preceding section (3.2), three cores No. 108, 118 and 144 exhibit deviations of the total gas content to smaller values (Fig. 4). Close-off densities for these three cores also deviate to larger values in Fig. 6. Deviations are too large to explain in terms of periodic fluctuations with depth in various parameters specifying the polycrystalline ice found by NARITA *et al.* (1978) in their structural study of the Mizuho core. Small value for No. 155 core reflects the fact that bubbles in this core have not been completely closed off. Omitting those four points stated above, we can draw a straight line as in Fig. 6 to express the altitude dependence of ρ_c .

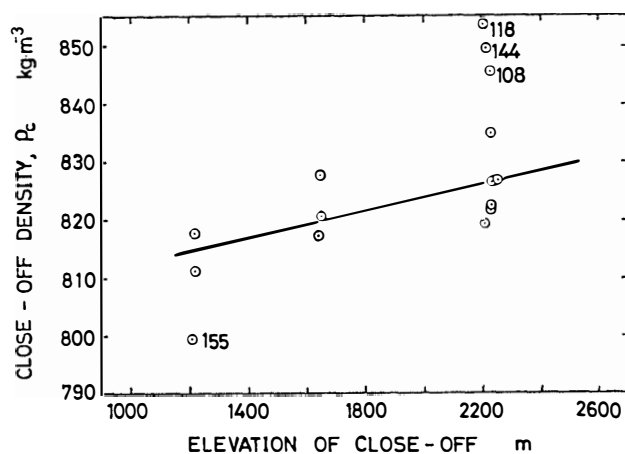


Fig. 6. Altitude dependence of the close-off density ρ_c .

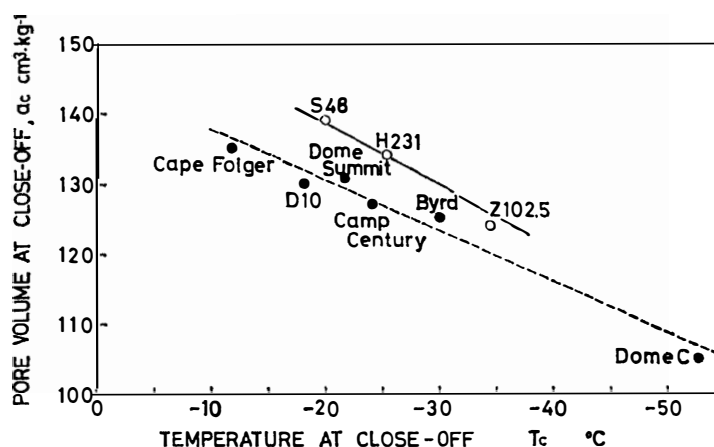


Fig. 7. Relationship between the void ratio a_c at close-off and the temperature of the sites of close-off.

Using the average values of ρ_c obtained from this straight line for three sites S 48, H 231 and Z 102.5, we can calculate the void ratio at the close-off a_c for each site by eq. (12). Calculated values of a_c are 139 (S 48), 134 (H 231) and 124 $\text{cm}^3 \cdot \text{kg}^{-1}$ (Z

102.5). They are correlated with the temperature of close-off sites as shown in Fig. 7 in which the results obtained by RAYNAUD and LEBEL (1979) for various places of the deep core drilling are also plotted. Our results exhibit a little higher level of a_c than that of RAYNAUD and LEBEL, although the inclination of temperature dependence is almost the same.

4.2. Total gas content and bubble pressure

The pressure difference between two sites of close-off for No. 102 core (55.4 m) and No. 261 (113.2 m) is only 3 mb as can be seen in a column of P_c of Table 3. Therefore, the decrease of the total gas content in ice with increasing depth as shown by a solid line in Fig. 4 can not be explained by the difference of P_c for the cores. Decrease of 3 mb at about 730 mb makes only 0.4% decrease of the total gas content, whereas the difference in Fig. 4 is approximately 12%. We have no explanation for this discrepancy at present but it could be an important clue to make clear mechanisms of bubble close-off in Antarctic ice sheets.

Figure 5 shows that bubble pressures in the ice core drilled at Z 102.5 are approximately 2 atmospheric pressure less than the overburden load pressure. Such difference was found with the results of Greenland (Site 2) ice cores even right after the core recovery (LANGWAY, 1958). Although the difference of approximately $2 \text{ kg} \cdot \text{cm}^{-2}$ never disappeared up to the bubble pressure $30 \text{ kg} \cdot \text{cm}^{-2}$ (31 atms.) in the above case, the bubble pressure seems to approach asymptotically to the overburden load pressure in the present case. In the case of the Z 102.5 site, they coincide at a depth of approximately 110 m. Since the accumulation rate of snow on the ice sheet in Mizuho Plateau is much less than that in Greenland, it is natural that the bubble pressure reaches the equilibrium with the overburden load pressure at a shallower depth in Mizuho than in Greenland. It will be interesting to correlate the depth where both pressures coincide to the accumulation rate of snow.

4.3. Errors and corrections

As described in the preceding section, measurements of both the density and the volume of air are accompanied by various types of systematic errors. The kerosine vapor correction and the dissolved air correction can be simply obtained by multiplying a certain factor to the measured volume of air and to the mass of specimens. Effects of surface-exposed air bubbles on the density and on the volume of air were described in Subsection 2.3, and it was found to be a difficult task to evaluate right corrections. It was shown in Fig. 3 that the correction for the density exceeded $5 \text{ kg} \cdot \text{m}^{-3}$ for ice cores at shallow depths of about 50–60 m. Corrections for the volume of air were in the order of several percent for specimens of smaller density as can be seen in Table 2. The surface corrections have never been paid attention by previous investigators and difference of the level of the void ratio a_c from other previous data shown in Fig. 7 may be attributed to these corrections, although there still remain some uncertainties of values derived from a large standard deviation of the accumulation rate.

Acknowledgments

We thank the members of JARE-15, -20 and -21 who made enormous efforts to recover ice cores, part of which were used in the present study. We thank Mr. Jun ASAI, a former student of our laboratory, for his efforts in constructing apparatus and obtaining preliminary data for the present study. Mr. H. TACHIBANA's kind help with the measurement of dissolved oxygen at the Water-Quality Engineering Laboratory of Hokkaido University is also acknowledged.

References

- BADER, H. (1964): Density of ice as a function of temperature and stress. *CRREL Spec. Rep.*, **64**, 6 p.
- HIGASHI, A. and HASHIMOTO, S. (1961): Mendenhōru Hyōga no chōsa (II) (The Mendenhall Glacier). *Shizen (Nature)*, **16**(3), 42–52.
- INOUE, M., YAMADA, T. and KOBAYASHI, S. (1977): Effects of synoptic scale disturbance on seasonal variations of katabatic winds and moisture transport into Mizuho Plateau. *Mem. Natl Inst. Polar Res., Spec. Issue*, **7**, 100–114.
- LANGWAY, C. C., Jr. (1958): Bubble pressures in Greenland glacier ice. *Physics of the Movement of the Ice: Symposium of Chamonix, Sept. 16–24, 1958. Gentbrugge, Association International d'Hydrologie Scientifique*, 336–349 (Publ. No. 47).
- MAENO, N. (1982): Densification rates of snow at polar glaciers. *Mem. Natl Inst. Polar Res., Spec. Issue*, **24**, 204–211.
- NAKAWO, M. (1980): Density of columnar-grained ice made in laboratory. *Division of Building Research, National Research Council of Canada*.
- NARITA, H. and MAENO, N. (1978): Compiled density data from cores drilled at Mizuho Station. *Mem. Natl Inst. Polar Res., Spec. Issue*, **10**, 136–139.
- NARITA, H., MAENO, N. and NAKAWO, M. (1978): Structural characteristics of firn and ice cores drilled at Mizuho Station, East Antarctica. *Mem. Natl Inst. Polar Res., Spec. Issue*, **10**, 48–61.
- NARUSE, R. (1978): Studies on the ice sheet flow and local mass budget in Mizuho Plateau, Antarctica. *Contrib. Inst. Low Temp. Sci., Hokkaido Univ., Ser. A*, **28**, 1–54.
- RAYNAUD, D. and LEBEL, B. (1979): Total gas content and surface elevation of polar ice sheets. *Nature*, **281**, 289–291.
- SATOW, K. (1978): Distribution of 10 m snow temperatures in Mizuho Plateau. *Mem. Natl Inst. Polar Res., Spec. Issue*, **7**, 63–71.
- SHIBUYA, K. and ITO, K. (1983): On the flow velocity of the ice sheet along the traverse route from Syowa to Mizuho Stations, East Antarctica. *Mem. Natl Inst. Polar Res., Spec. Issue*, **28**, 260–276.
- SUZUKI, Y. and SHIRAISHI, K. (1982): The drill system used by the 21st Japanese Antarctic Research Expedition and its later improvement. *Mem. Natl Inst. Polar Res., Spec. Issue*, **24**, 259–273.
- SUZUKI, Y. and TAKIZAWA, T. (1978): Outline of the drilling operation at Mizuho Station. *Mem. Natl Inst. Polar Res., Spec. Issue*, **10**, 1–24.
- WATANABE, O. (1977): Position and elevation of stations along the highland traverse and items of observation conducted there, 1974–1975. *JARE Data Rep.*, **36** (Glaciol. 4), 7–14.
- YAMADA, T. and WAKAHAMA, G. (1981): The regional distribution of surface mass balance in Mizuho Plateau, Antarctica. *Mem. Natl Inst. Polar Res., Spec. Issue*, **19**, 307–320.
- YAMADA, T. and WATANABE, O. (1978): Estimation of mass input in the Shirase drainage basins in Mizuho Plateau. *Mem. Natl Inst. Polar Res., Spec. Issue*, **7**, 182–197.

(Received May 4, 1983; Revised manuscript received August 6, 1983)